Lebensm.-Wiss. u.-Technol., 30, 70–76 (1997)

Simulation of Freezing or Thawing Heat Conduction in Irregular Two-dimensional Domains by a Boundary-fitted Grid Method

A.N. Califano and N.E. Zaritzky*

Centro de Investigación y Desarrollo en Criotecnología de Alimentos, CONICET, Facultad de Ciencias Exactas, Universidad Nacional de La Plata, 47 y 116 (1900) La Plata (Argentina)

(Received June 21, 1995; accepted March 18, 1996)

An alternative approach to the finite element method has been developed to simulate freezing and thawing processes in irregular two-dimensional systems. A code employing boundary-fitted grids (BFG) was implemented in a numerically conservative form (control volume formulation). The proposed model was satisfactorily checked against experimental data obtained with minced meat and Tylose. The accuracy of the BFG method is similar to one obtained by finite elements but shorter computer times and simpler codes were employed.

Keywords: computer simulation; freezing; thawing; mathematical modeling; irregular shapes; boundary fitted grid method

Introduction

It is difficult to model freezing and thawing processes because latent heat is released or absorbed over a range of temperatures. A more realistic model for freezing of solid biological materials is that of heat conduction with variable thermal properties. Chilling and freezing time prediction methods are often classified as: numerical methods and simple formulae. Numerical methods are generally considered the most realistic and versatile approach (1–4). They make discrete mathematical approximations to the time and spatial variations, defined by the governing partial differential equations for heat conduction. Finite differences and finite elements schemes are generally used. Traditionally, finite differences was considered a simpler method that led to satisfactory results for regular geometries (5–10), while finite elements method was more adequate for taking into account irregular multi-dimensional shapes (11–15). Finite elements needs large computer programs and computer facilities, requiring long processing times.

An alternative approach is the boundary-fitted grid method that employs a well behaved transformation in order to generate a nonuniform grid adapted to the irregular domain boundaries (16–18). This method allows use of a fully conservative numerical scheme like the control volume formulation (19) or subdomain method, which is a variant of the method of weighted residuals. In Patankar's own words (19): 'In the finite-element method and in most weighted-residual methods the assumed variation of the dependent variable consisting of the grid-point values and the interpolation functions between the grid points is taken as the approximate solution. In the finite-difference method, however, only the grid-point values of the dependent variable are considered to constitute the solution, without any explicit reference as to how it varies between the grid points'.

The objectives of the present study were: (i) to numerically simulate freezing processes in two-dimensional systems of arbitrary shape through the implementation of a conservative boundary-fitted grid code using variable thermophysical properties, and (ii) to compare the calculated freezing times with a set of experimental data obtained for minced beef and Tylose and predicted values by finite element method.

Mathematical Model

The governing equation for unsteady two-dimensional heat conduction in solids may be written as follows:

$$\rho \; Cp \frac{\partial T}{\partial t} = \frac{\partial}{\partial x}\left(k \frac{\partial T}{\partial x}\right) + \frac{\partial}{\partial y}\left(k \frac{\partial T}{\partial y}\right) \qquad \text{Eqn [1]}$$

When the integration domain has an irregular shape, the proposed procedure for the solution of this problem is to change coordinates conveniently; it is possible, in

*Also at Departamento Ingeniería Química, Facultad de Ingenería, UNLP.

0023-6438/97/010070 + 07$25.00/0/fs960130 ©1997 Academic Press Limited

general, to map conformally arbitrary regions into regular ones in the plane. Thus, the Cartesian coordinates **x, y** of the irregular domain L(x,y) are used in the initial frame system when the problem is posed mathematically. Then, by a general mapping U = U (x, y), V = V (x, y), the physical plane is mapped onto a rectangle in the curvilinear coordinate plane U, V. The irregular domain L(x,y) is transformed into a regular one L'(U,V), where a one-to-one correspondence between the points of both domains specifies a pointwise defined coordinate transformation as follows:

$$x,y \equiv x,y\ (U,V) \Leftrightarrow U,V \equiv U,V\ (x,y)$$

It is useful to employ a well behaved transformation in order to generate a nonuniform grid adapted to the domain boundaries. In the present work, boundary-fitted grids were generated by solving Laplace's equations for the fitted coordinates, namely (20):

$$\frac{\partial^2 x}{\partial U^2} + \frac{\partial^2 x}{\partial V^2} = 0$$

Eqn [2]

$$\frac{\partial^2 y}{\partial U^2} + \frac{\partial^2 y}{\partial V^2} = 0$$

with boundary conditions x = P (U, V); y = Q (U, V). In these expressions P and Q define the coordinates of the various body boundaries.

The original Eqn [1] was transformed in terms of the new coordinates U,V as follows:

$$\rho C p J \frac{\partial T}{\partial t} = \frac{\partial}{\partial U}\left[kJ\left(\frac{\partial T}{\partial U}AUU + \frac{\partial T}{\partial V}AUV\right)\right] + \frac{\partial}{\partial V}\left[kJ\left(\frac{\partial T}{\partial U}AVU + \frac{\partial T}{\partial V}AVV\right)\right] \quad \text{Eqn [3]}$$

where J is the Jacobian of the transformation and the coefficients shown in Eqn (3) are defined by:

$$J = \frac{\partial x}{\partial U}\frac{\partial y}{\partial V} - \frac{\partial x}{\partial V}\frac{\partial y}{\partial U} \quad \text{Eqn [4]}$$

$$AUU = \left(\frac{\partial U}{\partial x}\right)^2 + \left(\frac{\partial U}{\partial y}\right)^2 \quad \text{Eqn [5]}$$

$$AVV = \left(\frac{\partial V}{\partial x}\right)^2 + \left(\frac{\partial V}{\partial y}\right)^2 \quad \text{Eqn [6]}$$

$$AUV = AVU = \frac{\partial U}{\partial x}\frac{\partial V}{\partial x} + \frac{\partial U}{\partial y}\frac{\partial V}{\partial y} \quad \text{Eqn [7]}$$

The mathematical formulation of the problem in curvilinear coordinates is more complicated because the numerical coefficients *AUU, AUV, AVV, AVU* enter the equations. However, the transition to a more universal reference frame allows orthogonal grids that are either uniform or nonuniform in one or both directions to be constructed for more complex domains in physical space (21).

An algebraic analog of Eqn [3] was obtained by application of the control-volume formulation and an explicit discretization scheme with respect to time (20). The calculation domain was divided into a number of nonoverlapping discrete control volumes such that there is one control volume surrounding each grid point. The resulting differential equation was integrated over each control volume. The most attractive feature of the control-volume formulation is that the resulting solution would imply that the integral conservation of energy is exactly satisfied over any group of control volumes, and, of course, over the whole calculation domain (19). Coefficients *AUU, AUV, AVU* and *AVV* were numerically evaluated at faces east (E), west (W), north (N) and south (S) of the control volume, respectively. The Jacobian affecting the time derivative was calculated at the centre of the cell. Jacobians affecting spatial derivatives were computed at the corresponding planes (N, S, E and W). Thermophysical properties were considered to be variable through their temperature dependence. Thermal conductivities were also evaluated at each control volume face, for example, at east face (E) it became:

$$k^E = 2\ ((k_{i,j})^{-1} + (k_{i+1,j})^{-1})^{-1} \quad \text{Eqn [8]}$$

where k_{ij} corresponded to the grid point situated to the left of face E, and $k_{i+1,j}$ to the material placed to the right. Both points were equidistant to the face being considered. This formulation is based on a correct evaluation of the heat flux through each of the control volume faces. Thermal conductivities were calculated in the same way for the remaining faces.

The initial condition was:

$$t = 0;\ T = T_0 \text{ for the complete domain}$$

In order to consider the existence of a heat transfer coefficient (h) at the interface (convective boundary condition), heat balances were formulated on control volumes at the solid–fluid interface, where conductive

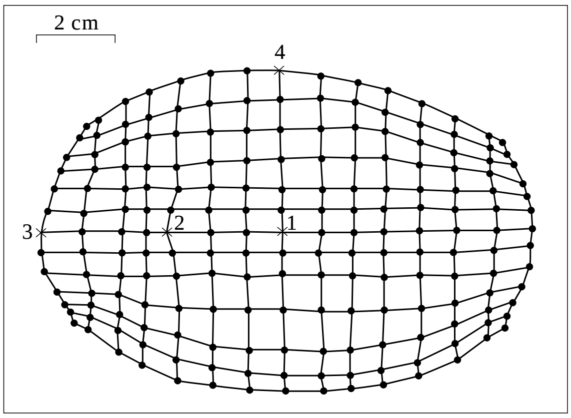

Fig. 1 Grid developed for the elliptical shape used in the experiments. × corresponds to thermocouple positions

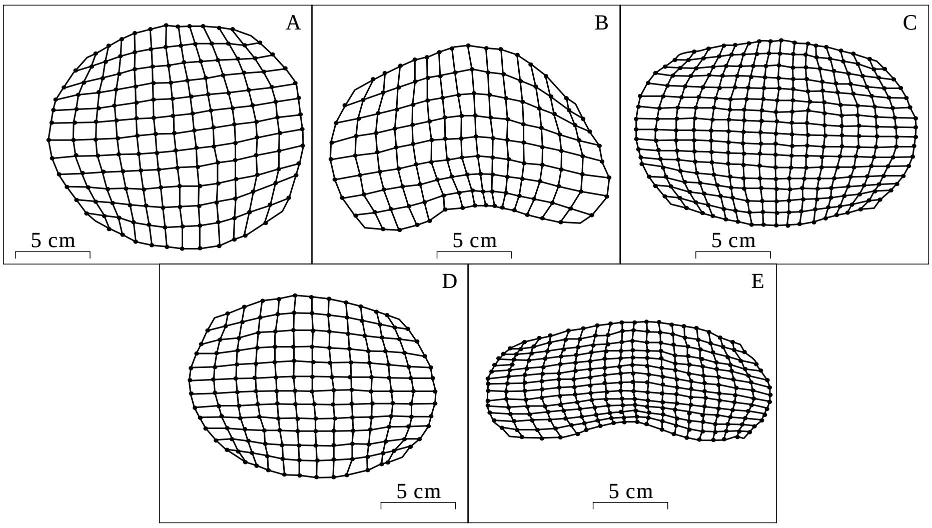

Fig. 2 Cross sections and fitted grids for shapes A, B, C, D and E used in the numerical simulations of Cleland *et al.* (22)

heat flux was replaced by convective heat flux on the appropriate faces.
Thus, a convective heat flux term for faces south (j = 1) and north (j = jmax) was:

$$q_{i,j} = h\ (T_f - T_{i,j})\ ARV_{i,j}\ J_{i,j} \qquad \text{Eqn [9]}$$

The arc length between two grid points, parallel to the north or south faces of the control volume situated at the solid–fluid interface ($ARV_{i,j}$) was calculated as:

$$ARV_{i,j} = \left[\left[\frac{\partial V}{\partial x}\right]^2_{i,j} + \left[\frac{\partial V}{\partial y}\right]^2_{i,j}\right]^{1/2} \qquad \text{Eqn [10]}$$

For west (i = 1) and east (i = imax) faces the appropriate arc length was:

$$ARU_{i,j} = \left[\left[\frac{\partial U}{\partial x}\right]^2_{i,j} + \left[\frac{\partial U}{\partial y}\right]^2_{i,j}\right]^{1/2} \qquad \text{Eqn [11]}$$

A code was written in Fortan ’77 and run in an PC/486DX2 computer with 4 Mb RAM.

Materials and Methods

Experimental thermal data in freezing and thawing processes were obtained for minced beef filling a cylindrical mould (30.8 cm length) with an elliptical cross section (12 × 7.7 cm). The two-dimensional elliptical shape and the grid used (11 × 11 nodes) in the prediction of the freezing and thawing times by the BFG method are shown in **Fig. 1**. The container was filled with minced lean beef (750 g/kg moisture, 30 g/kg fat) and copper–constantan thermocouples were suitably placed for recording time–temperature changes (**Fig. 1**). Polystyrene foam insulation was placed on the ends of the cylinder to reduce axial heat flow to an insignificant amount. The filled shape was placed in a constant-temperature freezer with stagnant air (–20 °C) for the freezing experiments. A constant-temperature

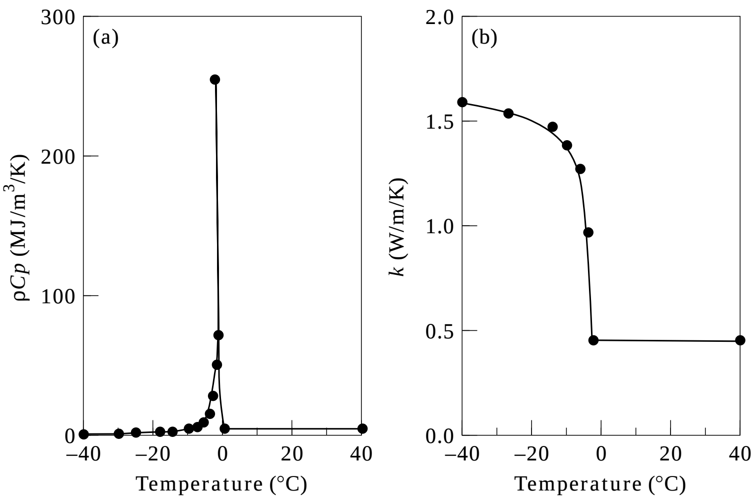

Fig. 3 Variation of (a) ρ Cp (density × specific heat) and (b) k (thermal conductivity) for lean beef. (●) corresponds to experimental data reported by Cleland *et al.* (23); (––) piecewise interpolation (present work)

storage room (20 °C) was used for the thawing runs (with air convection).

Heat transfer coefficients for freezing and thawing were determined a priori using an acrylic cylindrical shape of the same equivalent diameter as the elliptical shape and similar experimental conditions.

Table 1 Comparison of predicted and experimental times for freezing and thawing of two-dimensional irregular Tylose shapes processed at different conditions

Shape	h (W/(m²·°C))	T_f (°C)	T_0 (°C)	t_{exp} (h)	t_{pred} (h)	% ∊
A	28.0	–19.8	19.5	9.31	9.60	3.1
		–26.9	20.1	7.13	7.14	0.14
		–30.5	32.8	6.90	6.92	0.29
		–38.5	13.4	4.63	4.84	4.5
		20.3	–11.2	10.17	10.64	4.6
		13.7	–19.9	14.47	14.39	–0.55
		8.4	–19.4	18.69	20.07	7.4
		5.6	–18.4	27.32	26.12	–4.4
B	28.0	–19.8	18.1	7.82	7.72	–1.3
		–27.1	19.9	6.17	5.74	–7.0
		–38.6	19.1	4.04	4.11	1.7
		20.1	–21.5	8.98	8.55	–4.8
		13.7	–32.5	12.28	11.42	–7.0
		8.4	–13.2	16.86	15.41	–8.6
		5.6	–9.5	21.19	19.88	–6.2
C	28.0	–19.7	31.8	9.53	9.51	–0.21
		–23.7	4.3	6.31	6.39	1.3
		–25.1	34.9	7.30	7.65	4.8
		–26.9	20.0	6.70	6.50	–3.0
		–38.6	1.8	3.96	3.88	–2.0
		40.6	–12.1	5.40	5.93	9.8
		20.3	–31.3	9.98	10.10	1.2
		13.7	–21.9	13.28	13.10	–1.4
		13.6	–17.2	13.11	13.02	–0.67
		5.6	–31.7	24.98	24.01	–3.9
D	34.2	–19.6	31.4	5.01	5.18	3.4
		–26.9	20.0	3.55	3.53	–0.56
		–30.6	22.0	3.21	3.17	–1.2
		–39.1	2.3	2.05	2.10	2.4
		40.4	–29.8	3.19	3.25	1.9
		20.2	–20.1	5.23	5.18	–0.96
		13.7	–20.9	7.14	6.82	–4.5
		5.5	–9.7	13.08	12.23	–6.5
E	34.2	–19.7	14.4	3.40	3.18	–6.5
		–27.1	19.4	2.65	2.40	–9.4
		–38.7	18.3	1.70	1.69	–0.59
	20.3	–22.1	2.9	3.87	3.73	–3.6
		–29.6	33.7	3.48	3.59	3.2
		–34.1	34.5	3.11	3.16	1.6
	34.2	40.6	–11.9	1.76	1.82	3.4
		20.6	–11.4	3.01	3.04	1.0
		13.7	–20.2	4.43	4.25	–4.1
		5.6	–15.1	7.99	7.86	–1.6
	20.3	15.6	–12.1	4.70	5.16	9.8
		8.1	–11.2	7.69	8.32	8.2
		5.3	–27.6	11.77	11.59	–1.5

t_{exp}=experimental times from Cleland *et al.* (22); t_{pred}= predicted times, present work.

A, B, C, D and E correspond to shapes 3, 4, 2, 6 and 8, respectively, from Cleland *et al.* (22).

Numerical Simulations

Numerical simulations of freezing and thawing processes were performed for two-dimensional irregular Tylose shapes which correspond to a large set of experimental data published by Cleland *et al.* (22). **Figure 2** shows the grids generated in the present work for these shapes.

Tylose – MH – 100 or ‘Karlsruhe test substance’, is a 23% gel made of methylhydroxyethyl cellulose. Its thermal properties are very similar to those of lean beef with 74% water.

Assessment of the prediction accuracy of the numerical methods was made by direct comparison of the numerically calculated times for the thermal centre temperature of the objects to reach –10 °C for freezing and 0 °C for thawing, with the experimentally measured times reported by Cleland *et al.* (22). Freezing and thawing times for minced lean beef (750 g/kg moisture, 30 g/kg fat) were also predicted. The grids of **Fig. 2** were used for the calculations, as well as the grid shown in **Fig. 1** which corresponds to the experiments performed in the present work and described above. The variation

Table 2 Comparison of predicted and experimental times for freezing and thawing of two-dimensional irregular minced beef shapes processed at different conditions

Shape	h (W/(m²·°C))	T_f (°C)	T_0 (°C)	t_{exp} (h)	t_{pred} (h)	% ∊
A	28.0	21.0	–27.1	10.07	10.78	7.1
		8.1	–13.2	19.50	19.68	0.92
		–29.1	18.8	6.27	6.76	7.8
		–30.2	24.5	6.33	6.81	7.6
E	20.3	–23.3	3.1	3.43	3.57	4.1
		–37.8	32.2	2.59	2.86	10.4
		13.9	–11.6	5.05	5.42	7.3
		6.5	–16.3	8.75	9.54	9.0

Shapes from Cleland *et al.* (22).

Table 3 Percentage differences between the experimental and predicted freezing and thawing times for Tylose and minced lean beef in two-dimensional irregular shapes

	Numerical method	ε Mean (%)	SD (%)
Freezing and thawing Tylose (46 runs)	BFG	–0.4	4.6
	FEM_f	0.3	5.1
	FEM_s	4.2	6.1
Freezing Tylose (22 runs)	BFG	–4.4	3.7
	FEM_f	–1.0	4.5
	FEM_s	2.6	4.8
Thawing Tylose (24 runs)	BFG	–0.4	5.3
	FEM_f	1.5	5.5
	FEM_s	5.8	7.0
Freezing and thawing Minced beef (8 runs)	BFG	6.8	3.0
	FEM_f	12.3	2.9

BFG=boundary-fitted grid method, this work; FEM_f=finite element method, full unmodified formulation (3); FEM_s= finite element method, simplified formulation (3).

of ρCp (density × specific heat) and *k* (thermal conductivity) with temperature for lean beef as reported by Cleland *et al.* (23), and the piecewise interpolation that was fitted in the present work by the computer code, are shown in **Fig. 3a** and **b**, respectively. A similar approach was used for the thermal properties of Tylose. The time step was kept smaller than 0.5 s in order to avoid the problem of 'jumping' of the sharp peak in the effective specific heat according to the recommendations of Cleland and Earle (2).

Predicted times obtained with the boundary-fitted grid method developed in the present work were compared to those obtained by finite elements methods, both simplified and full unmodified formulations (3) for the same geometrical systems and experimental conditions.

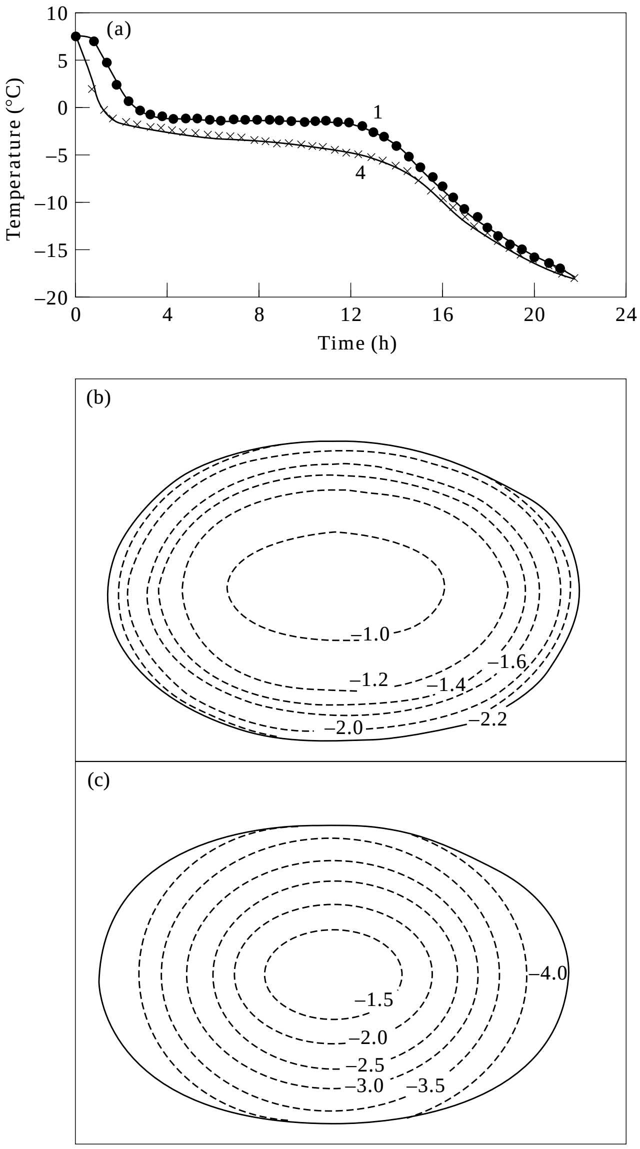

Fig. 4 Freezing of minced lean beef: h = 6.0 W/(m^2·K); T_f = –20.0 °C; T_0 = 7.5 °C. (a) Comparison of temperature profiles for the thermocouples located at positions 1 (centre) and 4 (surface) shown in **Fig. 1**. (b,c) Isothermal field at processing times of 4 h, (b) and 10 h (c). Numbers in isotherms correspond to temperature in °C

Results and Discussion

Tables 1 and **2** show predicted freezing and thawing times for Tylose and minced beef, respectively, processed at different conditions. Experimental data reported by Cleland *et al.* (22) and percentage differences are also included in these tables. As can be observed in **Table 3**, average percentage difference for freezing and thawing times was –0.4% in the case of Tylose. Accurate predictions of these times (within the tolerances allowed for experimental error) were obtained for all tested shapes. For minced beef the average percentage difference was 6.8%, which was higher than for Tylose. According to Cleland *et al.* (3) this can be attributed to a systematic error in the estimation of the surface heat transfer coefficient.

Percentage differences obtained by Cleland *et al.* (3) using finite element are also included in **Table 3**. The obtained errors with the boundary-fitted grid method (present work) were similar to those calculated by the full unmodified formulation of the finite element method.

In order to simulate thermal profiles in the cylindrical shape with an elliptical cross section the heat transfer coefficient of the system described in the above section was determined as the one that gave a minimum sum of squared deviations between the predicted and measured temperatures in the experiments performed with cylindrical shapes. The obtained values were h = 6.0

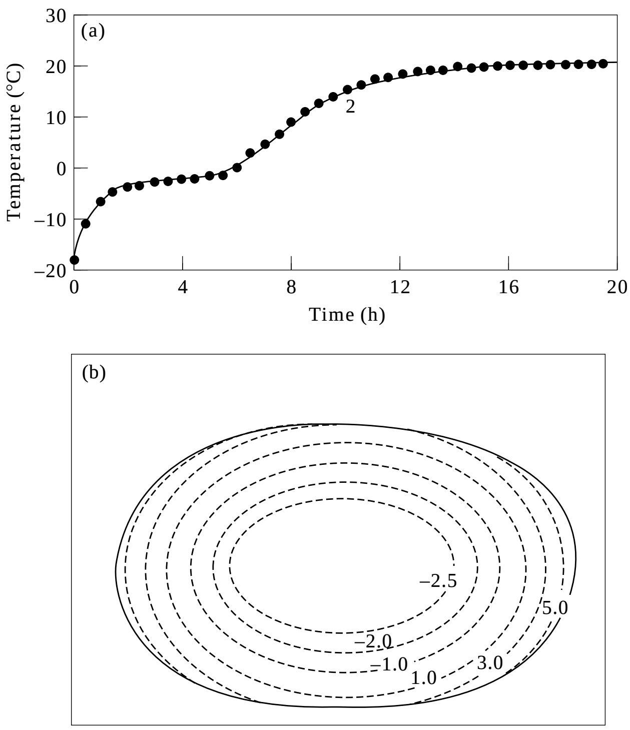

Fig. 5 Thawing of minced lean beef: h = 14.0 W/(m^2·K); T_f = 20.0 °C; T_0 = –18.0 °C. (a) Comparison of temperature profiles for thermocouple number 2 shown in **Fig. 1**. (b) Isothermal field at 4 h. Numbers in isotherms correspond to temperature in °C

W/(m^2·K) and h = 14 W/(m^2·K) for freezing and thawing conditions, respectively.

Typical predicted temperature profiles obtained by the BFG method were compared with those measured, both for freezing and thawing experiments. (**Figs 4a** and **5a**). Very good agreement was found between predicted and experimental temperatures at each measured point. Relative errors in the predicted temperatures did not exceed 3%. Computer isotherm curves during freezing (**Fig. 4b,c**) and thawing (**Fig. 5b**) were also obtained in the present work.

Conclusions

Boundary-fitted grid is an adequate method that can be applied to predict freezing and thawing times in irregular shaped food. Its accuracy is similar to that of the full unmodified finite elements formulation; oscillations in the solution were not produced even with an explicit time scheme; computer memory requirements were much lower than in FEM methods; simple codes can be developed without the need for using commercial programmes; very short computer times and small memory requirements (less than 520 Kb) were necessary; heterogeneous systems with different thermal properties can be modelled; agreement between numerical solution and experimental data was very good.

Acknowledgements

The financial support of the Consejo Nacional de Investigaciones Cientificas y Tecnicas (CONICET), Argentina, is gratefully acknowledged. Authors also express appreciation to J.C. Ferreri for his help in project execution.

Nomenclature

AUU, *AVV*, *AUV*, *AVU* = Coefficients defined in Eqns [5] to [7]
ARU, *ARV* = Arc lengths defined in Eqns [11] and [10], respectively
Cp = Specific heat (J/(kg·K))
h = Heat transfer coefficient (W/(m^2·K))
J = Jacobian of the transformation
k = Thermal conductivity (W/(m·K))
q = Heat flux (W/m^2)
t = Time (s)
T = Temperature (°C)
T_f = Temperature of the surrounding fluid (°C)
T_0 = Initial temperature of the object (°C)
ΔT = Temperature difference between the object of the surrounding fluid (°C)
U, V = Reference coordinates in the computational plane
x, y = Spatial coordinates of the irregular domain

Greek letters
ρ = Density (kg/m^3)
% ε = ((Predicted time – Experimental time)/Experimental time) $\times$ 100

Superscripts
E, W, N, S = Corresponds to faces east, west, north and south, respectively

Subscripts
i, *j* = grid coordinates

References

1 Heldman, D. R. Factors influencing food freezing rates. *Food Technology*, **37** (4), 103–109 (1983)
2 Cleland, A. C. and Earle, R. L. Assessment of freezing time prediction methods. *Journal of Food Science*, **49**, 1034–1042 (1984)
3 Cleland, D., Cleland, A. C., Earle, R. L. and Byrne, S. Prediction of freezing and thawing times for multi-dimensional shapes by numerical methods. *International Journal of Refrigeration*, **10**, 32–39 (1987)
4 Cleland, A. C. *Food Refrigeration Processes, Analysis Design and Simulation*. London: Elsevier Applied Science, pp. 33–77 (1990)
5 Bonacina, C. and Comini, G. On a numerical method for the solution of the unsteady state heat conduction equation with temperature dependent parameters. *Proceedings of the 13th International Congress of Refrigeration*, **2**, 329–336 (1971)
6 Bonacina, C. and Comini, G. On the solution of the non-linear heat conduction equations by numerical methods. *International Journal of Heat and Mass Transfer*, **16**, 581–589 (1973)
7 Mascheroni, R. H. and Calvelo, A. A. A simplified model for freezing time calculations in foods. *Journal of Food Science*, **47**, 1201–1207 (1982)
8 Succar, J. and Hayakawa, K. Parametric analysis for predicting freezing time of infinitely slab-shaped food. *Journal of Food Science*, **49**, 468–477 (1984)
9 Pham, Q. T. A fast, unconditionally stable finite-difference scheme for heat conduction with phase change. *International Journal of Heat and Mass Transfer*, **28**, 2079–2084 (1985)
10 Wilson, H. A. and Singh, R. P. Numerical simulation of individual quick freezing and spherical foods. *International Journal of Refrigeration*, **10**, 149–155 (1987)
11 Cleland, A. C. A review of methods for predicting the duration of freezing equipment. In: Le Maguer, M. and Jelen, P. (Eds), *Food Engineering and Process Applications*, Vol.2. London: Elsevier Applied Science, pp. 41–54. (1986)
12 Comini, G., Del Giudice, S., Lewis, R. W. and Zienkiewicz, O. C. Finite element solution of non-linear heat conduction problems with special reference to phase change. *International Journal for Numerical Methods in Engineering*, **8**, 613–624 (1974)
13 Rebellato, L., Del Giudice, S. and Comini, G. Finite element analysis of freezing processes in foodstuffs. *Journal of Food Science*, **43**, 239–250 (1978)
14 Purwadaria, H. K. and Heldman, D. R. A finite element model for prediction of freezing rates in food products with anomalous shapes. *Transactions of the ASAE*, **25**, 827–831 (1982)

15 Pan, J. C. and Bhowmik, S. R. The finite element analysis of transient heat transfer in fresh tomatoes during cooling. *Transactions of the ASAE*, **24**, 972–976 (1991)
16 Fiora, A. and Ferreri, C. Computation of steady nonlinear heat conduction in domains of arbitrary shape by means of discrete coordinate transformations. *Latin American Journal of Heat and Mass Transfer*, **2**, 29–44 (1978)
17 Ferreri, C. and Ventura, M. A. On the accuracy of boundary fitted finite-difference calculations. *International Journal for Numerical Methods in Fluids*, **4**, 359–375 (1984)
18 Grandi, G. M. and Ferreri, C. On the solution of heat conduction problems involving heat sources via boundary-fitted grids. *Communication in Applied Numerical Methods*, **5**, 1–6 (1989)
19 Patankar, C. V. *Numerical Heat Transfer and Fluid Flow*. New York: McGraw Hill Book Co., pp. 25–74 (1980)
20 Califano, A. N. and Zaritzky, N. E. A numerical method for simulating heat transfer in heterogeneous and irregularly shaped foodstuffs. *Journal of Food Process Engineering*, **16**, 159–171 (1993)
21 Dar'in, N. A. and Mazhukin, V. I. Modeling two-dimensional unsteady-state problems on grids with dynamic adaptation. *Mathematical Modeling and Computational Experiment*, **1**, 301–315 (1993)
22 Cleland, D., Cleland, A. C., Earle, R. L. and Byrne, S. Experimental data for freezing and thawing of multidimensional objects. *International Journal of Refrigeration*, **10**, 22–31 (1987)
23 Cleland, D., Cleland, A. C., Earle, R. L. and Byrne, S. Prediction of thawing times of simple shaped foods. *International Journal of Refrigeration*, **9**, 220–228 (1986)